cIAP1 regulates TNF-mediated cdc42 activation and filopodia formation

Arthur MARIVIN*[1,2], Jean BERTHELET*[1,2], Jessy CARTIER[1,2], Catherine PAUL[2,4], Simon GEMBLE [1,2], Alexandre MORIZOT[3], Wilfrid BOIREAU[5], Maya Saleh[3], Jacques BERTOGLIO[6, 7], Eric SOLARY[7,8] and Laurence DUBREZ[1,2]

From: Institut National de la Santé et de la Recherche Médicale (Inserm) UMR866, Dijon, F-21079, France[1]; Université de Bourgogne; Institut Fédératif de Recherche (IFR) 100, Dijon, F-21079, France[2] ; Department of Medicine, McGill University, Montreal, Quebec, Canada[3] ; *Ecole Pratique des hautes études (EPHE), Dijon, F-21079, France[4],* Institut FEMTO-ST, Université de Franche-Comté, CLIPP, 25044 Besançon, France[5], *Inserm UMR749[6] and UMR1009[8], Institut Gustave Roussy[7], Villejuif, F-94805, France; Institut Fédératif de Recherche (IFR) 54, Villejuif, F-94805, France[7]*

*Both authors contributed equally to this work.

Address correspondence to: Laurence Dubrez, Inserm UMR866, Faculty of Medicine, 7 Boulevard Jeanne d'Arc, 21079 Dijon cedex, France. E-mail: ldubrez@u-bourgogne.fr; Tel: (33) 380 393 356; Fax: (33) 380 393 434

Running title: cIAP1 regulates cdc42.

Keywords: IAPs, TNF, RhoGTPases, cdc42, metastasis, Ras.

Abstract

Tumor necrosis factor α (TNF) is a cytokine endowed with multiple functions, depending on cellular and environmental context. TNF receptor engagement induces the formation of a multimolecular complex including the TNFR-associated factor TRAF2, the receptor-interaction protein kinase RIP1, and the cellular inhibitor of apoptosis cIAP1, the latter being essential for NF-κB activation. Here, we show that cIAP1 also regulates TNF-induced actin cytoskeleton reorganization through a cdc42-dependent, NF-κB-independent pathway. Deletion of cIAP1 prevents TNF-induced filopodia and cdc42 activation. The expression of cIAP1 or its E3-ubiquitin ligase defective mutant restores the ability of cIAP1$^{-/-}$ MEFs to produce filopodia, whereas a cIAP1 mutant unable to bind TRAF2 does not. Accordingly, the silencing of TRAF2 inhibits TNF-mediated filopodia formation whereas silencing of RIP1 does not. cIAP1 directly binds cdc42 and promotes its RhoGDIα-mediated stabilization. TNF decreases cIAP1-cdc42 interaction, suggesting that TNF-induced recruitment of cIAP1/TRAF2 to the receptor releases cdc42 that, in turn, triggers actin remodeling. cIAP1 also regulates cdc42 activation in response to EGF and HRas-V12 expression. A downregulation of cIAP1 altered the cell polarization, the cell adhesion to endothelial cells and cell intercalation, which are cdc42-dependent processes. Last, we demonstrated that the deletion of cIAP1 regulated the HRas-V12-mediated transformation process, including anchorage dependent cell growth, tumor growth in a xenograft model and the development of experimental metastasis in the lung.

Keywords: IAPs, TNF, RhoGTPases, cdc42, metastasis, Ras.

Introduction:

Tumor necrosis factor α (TNF) is a mediator of immune and inflammatory response produced by activated monocytes and macrophages. This cytokine promotes cell proliferation, cell differentiation, cytokine secretion, and cell death, depending on the cellular and environmental context (1). TNF also affects cell shape and cell movement, which may contribute to the recruitment of fibroblasts or neutrophils to the site of tissue injury (2). Such morphogenetic modifications involve a dynamic rearrangement of the actin cytoskeleton controlled by small GTPases of the Rho family that includes rhoA, rac1, and cdc42. For example, in endothelial cells, TNF induces the sequential activation of rac1, rhoA, and cdc42 which lead to the formation of stress-fibers and cell contraction (2, 3). In fibroblasts and macrophages, TNF triggers the activation of cdc42 that is responsible for the transient formation of the actin-rich protrusions known as filopodia (2, 4, 5). Rho GTPases act as molecular switches that transduce the signal from membrane receptors to downstream effectors through shuttling between a GTP-bound active state and a GDP-bound inactive state. Once activated, they are either rapidly recycled into the inactive form or degraded by the ubiquitin-proteasome machinery. The Rho GTPase activation cycle is controlled by guanine-nucleotide exchange factors (GEFs), which catalyse the transfer of GDP-bound forms into GTP-bound forms; GTPase-activation proteins (GAPs) which inactivate Rho GTPases by hydrolysing the GTP; and guanine-nucleotide dissociation inhibitors (GDIs), which are chaperones that stabilize Rho GTPases in a cytosolic inactive state (2, 6, 7).

TNF binds two related membrane surface receptors. TNFR1, whose expression is ubiquitous, mediates most of the biological effect of the cytokine, whereas TNFR2 expression is restricted mostly to lymphocytes and endothelial cells. Upon ligand stimulation, TNFR1 recruits, in a membrane-associated complex, the cytosolic adaptor TNFR1-associated death domain protein (TRADD), the TNFR-associated factors (TRAFs), the receptor-interaction protein kinase 1 (RIP1), and the cellular inhibitors of apoptosis (cIAPs) (8-11). This molecular platform activates ubiquitin-dependent signaling pathways, leading to the nuclear factor-kappaB (NF-κB), the mitogen-activated protein kinase (MAPK) activations, and the expression of genes encoding for cytokines, adhesion molecules, survival, and differentiation factors (11-13). In the absence of cIAPs or when the NF-κB signaling is blocked, secondary cytoplasmic complexes leading to cell death are generated from the first one (14-17).

cIAPs, including cIAP1 and cIAP2, are E3-ubiquitin ligases as a result of the presence of a C-terminal RING domain. In addition to the RING, they own three baculovirus IAP repeat (BIR) domains mediating protein-protein interactions, an ubiquitin-binding associated (UBA) domain that allows the

recruitment of cIAPs into protein complexes (18) and a caspase recruitment domain (CARD) that regulates the E3 activity of the RING domain (19). Numerous ubiquitination targets and/or partners of cIAP1 have been identified, including signaling molecules, regulators of NF-κB activating pathways (20), and transcriptional regulators such as Mad1 (21) and E2F1 (22). In the TNFR1 signaling pathway, cIAP1 promotes its own ubiquitination and the ubiquitination of the kinase RIP1 required for NF-κB activation and survival, while it inhibits the formation of the RIP1-containing secondary intracellular platforms that trigger cell death (9, 11, 12, 14-16). cIAP1 is also a potent inhibitor of the alternative NF-κB activating pathway through ubiquitination leading to degradation of NIK (23, 24).

The present study demonstrates that cIAP1 also regulates filopodia formation in response to TNF, EGF and oncogenic HRas-V12 expression. cIAP1 directly interacts with cdc42 and regulates its activity by promoting its RhoGDI-mediated stabilization. We show that TNF stimulation disrupts the cIAP1/cdc42 interaction, and facilitates cdc42-mediated actin rearrangement, independently of NF-κB activation. A downregulation of cIAP1 affected cdc42-regulated processes including cell polarization, cell adhesion, cell intercalation and HRas-V12-mediated cell transformation.

Results

Deletion of cIAP1 alters actin cytoskeleton organization.

A previous work from Oberoi *et al*. (25) demonstrated that murine embryonic fibrobasts (MEFs) from *birc2*-deficient mice (cIAP1$^{-/-}$) displayed an altered morphology compared to the wild-type counterparts. Accordingly, serum-starved cIAP1$^{-/-}$ MEFs exhibited elongated and contracted cell bodies and the presence of subtle fine extended protrusions similar to filopodia (Figure 1A), an effect quantified by counting cells harboring more than five filopodia-like structures (Figure 1B). Filopodia is specifically controlled by the RhoGTPase cdc42 (6). The expression of cIAP1 or a dominant negative form of cdc42 (cdc42-N17) abolished the filopodia-like structures in cIAP1$^{-/-}$ MEFs (Figure 1B and C), demonstrating a cdc42-dependent phenomenon. The adaptor TRAF2 is a well-known partner of cIAP1 that is required for cIAP1 recruitment into TNFR complex. The expression of cIAP1^{L47A} mutant, which cannot interact with TRAF2 (22)(Supplementary Figure 1), or the E3-ubiquitin ligase activity defective mutant (cIAP1^{H588A}), also impeded filopodia-like formation (Figure 1B and C). Depletion of cIAP1 leads to a stabilization of the NF-κB-inducing kinase NIK and a constitutive activation of NF-κB (17, 26). Neither the silencing of NIK or the expression of IκB-super repressor (IκB-SR) significantly

abolished spontaneous filopodia in cIAP1$^{-/-}$ MEFs (Figure 1B and C). The expression of IκB-super repressor (IκB-SR) did not either alter the capacity of cIAP1 to suppress filopodia (Figure 1B and C), demonstrating that the reorganization of actin cytoskeleton in cIAP1$^{-/-}$ MEFs was independent of NF-κB activation.

cIAP1 mediates cdc42 stabilization through RhoGDIα

A western blot analysis of Rho GTPases demonstrated a reduced expression of cdc42 in cIAP1-depleted cells (Figure 2A and B). However, the GTP-bound / total cdc42 ratio was increased (Figure 2B and C), demonstrating a constitutive activation of cdc42, which was associated with an increase in the phosphorylation of the direct cdc42 effector PAK1 (Figure 2C). Once activated, RhoGTPAses can be degraded by the proteasome system. The proteasome inhibitor MG132 prevented the down-regulation of cdc42 (Figure 2A and B). Conversely, overexpression of cIAP1 in NIH3T3 or restoration of cIAP1 in cIAP1$^{-/-}$ MEF increased the cdc42 total level (Figure 2D and E, Supplementary Figure 2), mostly in the cytosolic enriched fraction (Figure 2F), and, to a lesser extent, the GTP-bound cdc42 (Figure 2D). In sum, our data suggest that cIAP1 could stabilize cdc42, mainly in its cytosolic inactive state. RhoGDIα is an important regulator of Rho GTPases that directly binds the proteins and stabilizes the cytosolic inactive forms (7, 27). Silencing of RhoGDIα prevented the cIAP1-mediated up-regulation of cdc42 (Figure 2E, Supplementary Figure 2), and overexpression of cIAP1 increased the proportion of RhoGDIα associated with cdc42, i.e. co-precipitation experiments showed that an equivalent quantity of RhoGDIα pulled down more cdc42 in cIAP1-overexpressing cells (Figure 2G), demonstrating the importance of RhoGDIα in cIAP1-mediated cdc42 stabilization.

cIAP1 interacts with cdc42.

We demonstrated an interaction of cIAP1 with cdc42, RhoA, and Rac1 in a glutathione S-transferase (GST) pull-down assay (Figure 3A). Similar results were obtained in a co-immunoprecipation experiment using Myc-cIAP1 and EGFP-Rho GTPases (Supplementary Figure 3A). Cdc42 bound to cIAP1 BIR-containing constructs (BIR1-3, BIR 1-2 and BIR 2-3), and to the single BIR2 domain with a high affinity, while TRAF2 bound to BIR1 (Figure 3B). Both GTP- and GDP-loaded cdc42 bound cIAP1, while only the GTP-form bound the cdc42 effector PAK1 (Figure 3C, Supplementary Figure 3B). These results were confirmed by using the Surface Plasmon Resonance technology (Biacore system) showing that the BIR domains of cIAP1 directly bound GDP and GTP-loaded recombinant cdc42 with an affinity quite similar (Figure 3D). An interaction of cdc42 with cIAP1, RhoGDIα and also TRAF2 was observed *in vivo* in co-immunoprecipitation experiments (Figure 3E).

The use of recombinant proteins demonstrated that cIAP1, but not TRAF2, could directly interact with cdc42. However, TRAF2 bound GST-cdc42 in the presence of cIAP1 (Figure 3F).

cIAP1 is required for TNF-induced filopodia formation and Cdc42 activation

In fibroblasts, TNF induces the activation of cdc42 leading to the formation of filopodia (4, 5, 28, 29). Accordingly, we observed filopodia in serum-starved NIH3T3 fibroblasts within 15 minutes of TNF treatment (Figure 4A and B). Simultaneously, TNF activated cdc42 and Rac1 Rho GTPases, as indicated by the appearance of GTP-bound Rho GTPases, and induced the dephosphorylation of the downstream effectors GSK3 (serine/threonine protein kinase glycogen synthase kinase-3) and the actin-binding protein cofilin (30) (Figure 4C). siRNA-mediated silencing of cIAP1 prevented the formation of filopodia (Figure 4A and B), the activation of cdc42 and Rac1, and the modifications of Rho GTPase downstream effectors (Figure 4C). cIAP2 siRNA also reduced TNF-induced reorganization of the actin cytoskeleton (Supplementary Figure 4). In MEFs, the TNF-induced filopodia were larger and more abundant compared to the spontaneous filopodia-like structures observed in cIAP1$^{-/-}$ MEFs (see Figure 1A and 5A), which was confirmed by counting the number of filopodia per cells (Figure 5B). TNF treatment did not induce the formation of new filopodia, and even significantly decreased spontaneous filopodia structures, in cIAP1$^{-/-}$ MEFs (Figure 5A and B), while a prolonged exposure induced cell death in cIAP1$^{-/-}$ MEFs but not in wt MEFs (17) (Supplementary Figure 5). We did not either observed filopodia formation in response to TNF in cIAP1/cIAP2 double knout-out MEFs (Figure 5C). The ability of cIAP1$^{-/-}$ MEFs to form filopodia in response to TNF was restored by the expression of wild-type cIAP1 as well as the E3-defective mutant cIAP1^{H588A} (Figure 5D and E). By contrast, cIAP1^{L47A} mutant did not restore TNF-induced filopodia formation in cIAP1$^{-/-}$ MEFs (Figure 5D and E) suggesting a role of TRAF2 in this process. Accordingly, silencing of TRAF2 in wt MEFs inhibited TNF-mediated filopodia formation (Figure 5F) while silencing of RIP1, which is the cIAP1-ubiquitin target in TNF signaling pathway, did not (Figure 5F). The TNF-mediated filopodia formation in cIAP1-reconstituted cIAP1$^{-/-}$ MEFs was totally inhibited by the expression of the dominant negative form of cdc42 (cdc42-N17), but was not affected by the expression of IκB-SR (Figure 5E). Overall, TNF induced filopodia formation via a cdc42-, cIAP1- and TRAF2-dependent but RIP1- and NF-κB-independent signaling pathway. Moreover, the cIAP1 E3-ubiquitin ligase required for TNF-induced ubiquitination of RIP1 and activation of NF-κB was dispensable. Of note, the expression of cIAP1^{L47A} mutant in wt MEFs inhibited TNF-induced filopodia formation (Figure 5E), suggesting a dominant negative effect. A co-immunoprecipitation experiment demonstrated that this mutant interacted with endogenous cIAP1 (Supplementary Figure 6).

We then analyzed the activation of cdc42, Rac1, and RhoA in response to TNF stimulation in MEFs (Figure 6A). As expected, TNF did not stimulate cdc42 in cIAP1$^{-/-}$ MEFs. The activation of Rac1, which occurs downstream of cdc42 in TNF-signaling pathway (4), was also abolished. The expression of the cIAP1^{L47A} mutant also decreased TNF-induced cdc42 activation and PAK1 phosphorylation, confirming the dominant negative effect of this mutant (Figure 6B). Altogether, our results suggested that cIAP1 is required for cdc42 activation in response to TNF. Co-immunoprecipitation experiments showed that TNF exposure decreased the interaction of cIAP1 and TRAF2 with cdc42 (Figure 6C).

Unlike TNF that induces cdc42-dependent Rac1 activation (4), EGF activates cdc42 and Rac1 in an independent manner. Deletion of cIAP1 inhibited EGF-induced cdc42, but not Rac-1 activation (Figure 6A). Moreover, deletion of cIAP1 did not alter serum-induced RhoA activation (Figure 6A), suggesting a specific regulation of cdc42 activation by cIAP1. The EGF-induced filopodia formation was abolished in cIAP1$^{-/-}$ MEF and was restored by the expression of cIAP1 (Supplementary Figure 7). Silencing of TRAF2 did not inhibit EGF-induced filopodia formation (Supplementary Figure 7) suggesting a general regulation of cdc42 by cIAP1 while TRAF2 regulated specifically the TNF-signaling pathway.

cIAP1 regulates cdc42 functions.

Next, we examined the importance of cIAP1 in the cellular functions of cdc42. cdc42 is a specific regulator of cell polarization (31, 32). A downregulation of cIAP1 significantly affected cell polarization, as evaluated by analyzing the Golgi apparatus reorientation to face the leading edge, five hours after fibroblast scratching (Figure 7A). cdc42 is also an important intermediate in the Ras-mediated cell anchorage-independent cell growth and transformation pathways (33-36). The expression of the oncogenic HRas-V12 induced the activation of cdc42, which was completely blocked in cIAP1$^{-/-}$ MEFs (Figure 7B). Deletion of cIAP1 significantly decreased HRas-V12-mediated cell growth in soft agar medium (Figure 7C,) inhibited the growth of tumor cells when subcutaneously injected in nude mice (Figure 7D) and delayed the apparition of lung cancer foci after injection of the cells into the tail vein (Figure 7E, Supplementary Figure 8).

Several steps of the metastatic process are controlled by RhoGTPases including the dissemination of tumor cells through the lymph or the blood, their adhesion to vessel endothelium and their subsequent migration through endothelium to colonize adjacent organs. A recent report from Reymond *et al.* demonstrated that the attachment of cancer cells to endothelial monolayer and their transendothelial migration is more specifically controlled by cdc42 (37). As demonstrated for

cdc42 (37), silencing of cIAP1 significantly reduced the adhesion of PC3 cells to HUVEC monolayer and their intercalation between endothelial cells (Figure 7F). We then analyzed the capacity of MEFs, untransformed or transformed by HRas-V12, to adhere to and to intercalate between endothelial cells (supplementary Figure 9). Accordingly with the presence of filopodia-like structures on the cell surface, the cIAP1$^{-/-}$ MEFs spontaneously adhered to the HUVEC monolayer, more strongly compare to the wt counterpart (Figure 7G, left panel). HRas-V12 expression stimulated the attachment of MEFs to HUVEC monolayer (Figure 7G, left panel). Both the adhesion and the intercalation were decreased in HRas-V12-transformed cIAP1$^{-/-}$ MEFs compared to HRas-V12/wt MEFs (Figure 7G).

Discussion

cIAP1 is a key determinant of cellular response to TNF. The protein is recruited to the TNFR1 through the adaptor TRAF2 and mediates the activation of the canonical NF-κB survival pathway while inhibiting the assembly of secondary cytoplasmic caspase-activating platform leading to cell death (20). We demonstrate here that cIAP1 also regulates actin cytoskeleton reorganization upon TNF stimulation through a cdc42-dependent, NF-κB-independent pathway. We propose a model (Figure 8) in which cIAP1 could regulates the cycle of cdc42 activation through stabilizing the interaction of cdc42 with its regulator RhoGDIα. The recruitment of TRAF2/cIAP1 to the TNF membrane receptor after TNF stimulation could release cdc42 and allow its activation, leading to the actin cytoskeleton reorganization.

In fibroblasts, TNF induces the rapid and transient formation of filopodia (38) which requires the Rho GTPase cdc42 (5, 39, 40). The pathway connecting the TNFR1 to Rho GTPases remains poorly understood but appeared to be independent on NF-κB and MAPK activation (5, 29, 38). Accordingly, we observed that TNF induced filopodia formation in the presence of an IκB super-repressor. TNFR engagement triggers the TRAF2-dependent recruitment of cIAP1, which induces an autoubiquitination and the ubiquitination of RIP1 necessary for NF-κB activation (20). We demonstrate that TNF-induced filopodia formation requires cIAP1 and TRAF2 while RIP1 and the E3-ubiquitin ligase of cIAP1 are dispensable, suggesting that the TNFR-associated complex can generate independent signaling pathways leading to NF-κB activation or filopodia formation. cIAP1 can directly bind to cdc42 while TRAF2 can bind cdc42 only in the presence of cIAP1. Both cIAP1 and TRAF2 co-precipitate with cdc42 in resting cells, and TNF-treatment decreased this interaction. Our hypothesis is that the recruitment of cIAP1/TRAF2 to TNFR makes cdc42 activation easier, leading to the actin

cytoskeleton reorganization (Figure 8). Secondary molecular events are likely required for the full activation of cdc42, as the activation of Rho GTPases requires a GEF. Vav is a Rac1-GEF in TNFα signaling in fibroblasts (29), and the GEF Ect2 has been involved in the TNF-like weak inducer of apoptosis (TWEAK)-induced cdc42 activation in glioblastoma (41), but their role in cdc42 activation has to be explored in this cell context.

cIAP1 appears to fine tune cdc42 activation. On one hand, cIAP1 deletion inhibits cdc42 activation in response to TNF and EGF stimulation and HRas-V12 expression; on the other hand, down-regulation of cIAP1 decreases the expression of the whole cdc42 in a proteasome dependent manner, but increases the expression of the activated fraction of cdc42. The down-regulation of cIAP1 also promotes the phosphorylation of PAK1, a cdc42 effector, and cIAP1$^{-/-}$ MEFs spontaneously form filopodia-like structures. Interestingly, RhoGDIα depletion infers similar modifications, including a decreased of cdc42 protein level that can be prevented by inhibiting the proteasome, and an increased ratio of active to total cdc42 (27). RhoGDIα is a Rho chaperone, i.e. it maintains a pool of cytoplamic GTPases in a GDP-bound inactive state and protects them from a proteasomal degradation (27, 42). The expression of cIAP1 increases the cytosolic cdc42 expression in a RhoGDIα-dependent manner, and enhances the fraction of the cdc42 bound to RhoGDIα. Overall, these data argue for a RhoGDIα-mediated regulation of cdc42 by cIAP1.

The regulation of RhoGTPases by IAPs is evolutionary conserved, i.e. it has been observed in Drosophila (43) and Zebrafish (25). Identical to RhoGDIs (42), cIAP1 (present work), XIAP (25), and DIAP1 (43) can bind to both GDP- and GTP-bound GTPases. DIAP1 controls Rac activity independently of its E3-ubiquitine ligase domain (43), while XIAP promotes the ubiquitination and degradation of the active, GTP-bound form of Rac1 (25). We observed an interaction of cIAP1 with Rac1, RhoA and cdc42. In our study, cIAP1 failed to ubiquitinate cdc42 (Supplementary Figure 10), suggesting that IAPs could differentially modulate various Rho GTPases. RhoA, Rac1 and cdc42 compete for the binding to and chaperoning by RhoGDIα and the stabilization of the interaction of one Rho GTPase with RhoGDIα favors the degradation of the others (27). cIAP1 becomes part of this crosstalk regulatory mechanism by stabilizing cdc42-RhoGDIα interaction (present work) and catalyzing the proteasomal-degradation of Rac1 (25). Moreover, an inhibition of the SUMOylation of RhoGDIα by XIAP has been described (44) and a recent study identified RhoGDI2 as a potential IAP neddylation substrate (45). As central regulators of Rho GTPase homeostasis, IAPs could regulate their sequential activation in many biological processes such as intracellular vesicular traffic, morphogenesis, tissue repair, cell shape, plasticity, polarization, adhesion and motility (42). In drosophila, overexpression of DIAP1 compensates the invalidation of rac in the control of border cell migration during oogenesis (43). In mammals, the depletion of cIAPs or XIAP alters the invasive properties of cancer cells

including their migration (19, 25, 44, 46), their adhesion to endothelium and their intercalation between endothelial cells, which can be related to the deregulation of Rho GTPase homeostasis (25, 43, 44).

Our results indicate a regulatory function for cIAP1 in cdc42-controlled filopodia formation, cell polarization and adhesion (39, 47). The contribution of cdc42 to some oncogenic processes (6), for example the HRas-V12-driven cell transformation (33, 35, 36) and metastatic invasion (37) may account for the anti-tumor activity of small molecules inhibitors of IAPs, such as Smac mimetics.

Material and Methods

Cell culture and treatments

Mouse embryonic immortalized (SV40) fibroblasts (MEF) wt and cIAP1$^{-/-}$ and cIAP1$^{-/-}$/cIAP2$^{-/-}$ (J. Silke, Melbourne, Australia), mouse NIH3T3 fibroblasts and HEK293T cells were cultured in DMEM medium (Lonza, Verviers, Belgium) supplemented with 10% fetal bovine serum (FBS) (Lonza). Cells were serum starved for 16 hours before stimulation with 100 ng/mL TNF or EGF (Shenandoah Biotechnology Inc, Warwick, PA, USA). MG132 (Millipore, Calbiochem, Billerica, MA, USA) was used at 40µM for four hours. PC3 cells were cultivated in RPMI-1640 medium (Lonza) supplemented with 10% FBS (Lonza). Primary HUVECs (Lonza) were maintained in EBM2 medium (Lonza).

Plasmid constructs, siRNAs, cell transfection and viral transduction

NIH3T3 fibroblasts were transfected using Lipofectamine 2000 (Life technologies, Invitrogen, Carlsbad, CA, USA), and MEFs and HEK293T using JET PEI (Polyplus transfection, Illkirch, France). Lipofectamine 2000 (Invitrogen) was used for the transfection of siRNA targeting mouse NIK (Thermo Fisher Scientific, Waltham, MA, USA), cIAP1, TRAF2, RIP1 or RhoGDIα (designed and provided by Qiagen, Venlo, The Netherlands). DNA constructs used were pCR3-Flag-cIAP1, pCR3-flag-cIAP1^{L47A}, pCI-cIAP1, pCI-cIAP1^{H588A} pCI-cIAP1^{L47A} (22), pGEX-cIAP1^{wt}, pGEX-cIAP1^{BIR1-3} (amino-acid 1-483), pGEX-cIAP1$^{CARD-RING}$ (amino-acid 452-618), pGEX–cIAP1^{BIR1-2} (amino-acid 1-258), pGEX-cIAP1^{BIR2-3} (amino-acid 181-363), pGEXcIAP1^{BIR1} (amino-acid 34-129), pGEX-cIAP1^{BIR2} (amino-acid 170-260), pGEX-cIAP1^{BIR3} (amino-acid 256-358) (48), pMT90-Myc-cdc42^{N17}, pCDNA-HA-cdc42^{WT}, pEGFP-cdc42, pEGFP-RhoA, pEGFP-Rac1, pGEX-RhoA, pGEX-Rac1, pGEX-cdc42, pRcCMV-IkB-SR and pBABE-HRas^{V12}. HRas-V12 expressing MEFs were generated by a retroviral transduction. Phoenix^{TM}-Eco cells (Invitrogen) which constitutively produced gag-pol and ecotropic envelope proteins were transfected using Jet PEI (Polyplus transfection) with pMSCV-HRas-V12. MEFs were transduced overnight with the retroviral-

containing supernatant supplemented with 1µg/mL of polybrene (Sigma-Aldrich, St-Louis, MO, USA). Populations of transduced cells were selected by puromycin exposure. The efficiency of infection was checked by a western blot analysis.

Immunofluorescence analysis of filopodia and cell polarity.

Cells were grown and transfected on a chamber slide (Labtek, Thermo Fisher Scientific, Nunc), serum starved for 16h, stimulated with TNF or EGF. Cells were then washed twice with pre-warmed PBS, fixed for 10 min in 4% paraformaldehyde/PBS, permeabilized using 0.1% triton X-100 (10 min) and saturated for 20 min in 2 % bovine serum albumin. Actin cytoskeleton was labeled with AlexaFluor488-Phalloidin (Invitrogen) in PBS/BSA 0.5% for 30 min. Cells were mounted on glass slides using FluorSave (Millipore, Billerica, MA, USA), and examined using a fluorescence (Nikon Eclipse 80i, Nikon, Champigly, France) or a confocal (Leica TCS SP2; Leica, Bron, France) microscope. Filopodia were quantified by counting cells displaying more than five filopodia or by counting the number of filopodia / cells. More than 100 cells were analyzed.

Cell polarity was assessed by an analysis of the Golgi apparatus orientation in a wound-scratch test. Briefly, after wounding, cell monolayers were fixed and subjected to nucleus and Golgi staining using Hoechst 33258 (Sigma-Aldrich) and AlexaFluor568-conjugated anti-GM130 (Becton, Dickinson and Company) respectively. The percentage of cells (>150) with their Golgi orientated toward the wound was evaluated.

Cellular extracts, cell fractionation, immunoprecipitation and western blot analysis

Cells were lysed in RIPA (Tris-HCl 50mM pH 7.5, NaCl 150mM, NP-40 1%, DOC 0.5%, SDS 0.1%) or Phospho (Tris-HCl 50mM pH 7.5, NaCl 100mM, NP-40 2%, Glycerol 10%, MgCl2 10mM, NaF 10mM, Sodium orthovanadate 1 mM, phosphatase inhibitor phosphatase 2 and 3) buffers complemented with EDTA-free protease inhibitor cocktail (Sigma-Aldrich). Primary antibodies used for western blotting were goat anti-cIAP1 (R&D Systems, Minneapolis, MN, USA), and GST (Rockland Immunochemicals, Philadelphia, Pennsylvania, USA), rabbit anti-GFP (Becton, Dickinson and Company, Franklin Lakes, NJ, USA), RhoGDIα (Santa Cruz Biotechnology Inc, Santa Cruz, CA, USA), PAK1, p-PAK1, Cofilin, p-Cofilin, GSK3α/β, p-GSK3α/β (Cell Signaling Technology Inc, Danvers, MA, USA), and TRAF2 (Millipore Corporation, Upstate, Billerica, Massachusetts, USA), and mouse anti-HA (Covance), Rac1 (Upstate), cdc42 (Becton, Dickinson and Company), RhoA (Cytoskeleton Inc, Denver, CO, USA), cIAP2, pan-cIAPs (R&D Systems, Cyclex), GM130 (Becton, Dickinson and Company) and HSC70 (Santa Cruz Biotechnology Inc). The western blot analysis was performed as previously described (22). Cell fractionation experiments were performed by using the Subcellular Protein

Fractionation Kit for Cultured Cells (Thermo Fisher Scientific) according to the manufacturer instructions.

For immunoprecipitations, cells were lysed in IP buffer (50 mM TrisHCl pH7.5, NaCl 100mM, NP-40 2%, Glycerol 10%, MgCl2 10mM, NaF 10mM, Sodium orthovanadate 1 mM protease inhibitor cocktail), incubated for 4h at 4°C in the presence of rabbit polyclonal anti-RhoGDIα or mouse anti-HA, and then for 1h in the presence of mixed A+G agarose beads (Millipore). Beads were washed in IP buffer and denaturated in Laemmli buffer 2X before immunoblot analysis.

Rho GTPase activation assays

Cells were lysed in GTPase buffer (Tris-HCl 50mM pH 7.5, NaCl 300mM, NP-40 2%, Glycerol 10%, 10mM MgCl2, protease inhibitor cocktail). The active forms of RhoA, rac1 or cdc42 were selectively pull-downed by GST-Rhotekin-Rho binding domain or GST-PAK1-CRIB domain fused to glutathione-Sepharose beads (GE Healthcare, Amersham Biosciences, Fairfield, CT, USA). Beads were washed three times, eluted in Laemmli 2X and precipitated GTP-RhoA or Rac or Cdc42 was detected by western blot analysis using an anti-RhoA or Rac1 or Cdc42 antibody.

GST-pull down assay

GST fusion proteins were produced in *Escherichia coli*, immobilized on glutathione-Sepharose (Amersham Biosciences) and incubated with either tagged-protein expressing HEK293T cells lysates or recombinant cIAP1, TRAF2 (SignalChem, Richmond, Canada). The pull-down proteins were revealed by a western blot analysis. Recombinant cIAP1 protein was produced using TNT-quick coupled transcription/translation system (Promega, Madison, WI, USA) accordingly to the manufacturer's instructions. For the analysis of the interaction with GDP or GTP-bound form of cdc42, GST-cdc42 or cdc42 from cell lysates were charged with GDP (1mM) or GTPγS (0.1mM) (Millipore) in 0.5M EDTA for 15 min at 30°C under agitation before the pull-down assay. The reaction was stopped by adding 60mM MgCl2.

Surface Plasmon Resonance (Biacore) analysis

Design and fabrication of homemade chips compatible with Surface Plasmon Resonance was routinely performed with the help of the MIMENTO technological platform, Besançon, France. The cIAP1-BIRs chips fabricated in this study consist in the covalent grafting of cIAP1 entities on chemically activated self-assembled monolayer following the procedure of protein chip building

recently published (49). This procedure was performed in a 10 mM acetate buffer (pH4.5) and led to a surface coverage of approximately 8 fmol/mm^2 of cIAP1-BIRs per spot. Biacore experiments were performed with the Biacore 2000 apparatus at 25°C with a flow rate comprised of between 2 and 30µl/min. Purified cdc42 was charged with GDP (1mM) or GTPγS (0.1mM) (Millipore) in 0.5M EDTA for 15 min at 30°C under agitation and injected into the Biacore. Protein-protein interaction was monitored using the Biacore 200 control software (GE-Healthcare), and analyzed using the Biaevaluation 3.2 RCI software (GE-Healthcare).

Soft agar colony formation

Cells (50,000 cells / well) were cultured in 0.45% agarose in growth media, layered on top of 0.75% agarose growth media in a six well dish. Colonies were counted under a light microscope 2–3 weeks post-plating. For each experiment, cells were seeded in triplicate and three fields per well were quantified.

Mouse tumoral models

Exponentially growing HRas-V12 and control-transduced MEF cells (1 x 10^6 /100 µL PBS) were s.c. injected into the flank of nude mice. Tumor growth was monitored by measurement with calipers in two perpendicular diameters, and tumor volumes were calculated using the formula $v=a^{2'}b/2$ (a<b). For the analysis of lung colonization, HRas-V12-transduced MEFs (1 x 10^6 /100 µL PBS) were injected into the tail veins of nude mice. The mice were sacrificed 2 weeks later, and the number of tumor foci at the lung surface was counted. Lungs were fixed and sections were hematoxylin and eosin stained and observed using the AxioZOOM V16 (Carl Zeiss, Oberkoren, Germany). The experiments were performed twice, *n* = 4 to 5 per group.

Cell adhesion and intercalation

Cell adhesion and intercalation assay were performed as previously described (37). Briefly, 130 000 CSFE labeled PC3 cells or MEFs were added onto confluent HUVECs in 24 wells plates, then washed twice with PBS. Cells were trypsinized and adherent cells were quantified using LSRII flow cytometer (Becton, Dickinson and Company). For the analysis of intercalation, 150 000 PC3 cells or MEFs were added onto confluent HUVECs in 6 well plates. Cells were monitored by time-laps microscopy in a humidified chamber at 37°C and 5% CO2 with an inverted microscope AxioVert 200M (Carl Zeiss) equipped with a motorized stage with a 10x objective lens and using AxioVison software (Carl Zeiss). Cells were tracked manually using AxioVision software and cells were considered as intercalated

when its shape was no more round, when it was no longer phase-bright and clearly part of the HUVECs monolayer, as shown in Supplementary Figure 9.

Stastitical analysis

Student's t test, ANOVA or the Mann-Whitney test was used for statistical analysis.

Conflict of Interest

The authors declare no conflict of interest.

Acknowledgements

We would like to thank Dr. J. Silke, Dr. E Lemichez, Dr. S. Gasman, Dr C.L. Day, Dr S. Ansieu, Dr R. Weil and S. Monier for kindly providing plasmids and cell lines. We are grateful to Lydie Desoche, Aziza Aznague, Cedric Seignez and Benoit Simon (FEMTO-ST, CLIPP platform) for their technical assistance. We thank A. Bouchot and B. Gasquet (CellImaP Imagery Facility), A. Hammann (Cytometry platform), V. Saint-Giorgio (Animal Facility), A. Oudot and B. Collin (Precilinal imagery platform, Georges-François Leclerc Center) for the use of the imagery, cytometry and animal facilities. We thank P. Meier, K. Rajalingam, J. Bréard, M. David and S. Ansieu for helpful discussions. This work was supported by grants from the "Comité de Côte d'Or of the Ligue Contre le Cancer" (LD), the "Association pour la Recherche sur le Cancer" (ARC to LD), the Association "Cent pour sang la Vie" (LD), the European Union and the "Conseil Régional de Bourgogne", a French Government grant managed by the French National Research Agency under the program "Investissements d'Avenir" with reference ANR-11-LABX-0021', and fellowships from the "Ministère de l'Enseignement Supérieur et de la Recherche" of France (to AM, JB, JC), ARC (JC) and the "Société Française d'Hématologie" (AM).

Author contribution

AM and JB performed most of the experiments and analysed data, JB performed the *in vivo* experiment and analysis. JC performed additional experiments and data analysis. CP and AM contributed to the *in vivo* analysis. SG and WB performed the biacore experiments and analysis, MS and JB provided valuable materials and expert evaluation. ES provided expert evaluation and

corrected the paper and LD conceived and supervised the project, analysed data and wrote the paper with input from all authors.

References

1. Parameswaran N, Patial S. Tumor necrosis factor-alpha signaling in macrophages. Crit Rev Eukaryot Gene Expr. 2010;20(2):87-103.
2. Mathew SJ, Haubert D, Kronke M, Leptin M. Looking beyond death: a morphogenetic role for the TNF signalling pathway. J Cell Sci. 2009 Jun 15;122(Pt 12):1939-46.
3. McKenzie JA, Ridley AJ. Roles of Rho/ROCK and MLCK in TNF-alpha-induced changes in endothelial morphology and permeability. J Cell Physiol. 2007 Oct;213(1):221-8.
4. Peppelenbosch M, Boone E, Jones GE, van Deventer SJ, Haegeman G, Fiers W, et al. Multiple signal transduction pathways regulate TNF-induced actin reorganization in macrophages: inhibition of Cdc42-mediated filopodium formation by TNF. J Immunol. 1999 Jan 15;162(2):837-45.
5. Puls A, Eliopoulos AG, Nobes CD, Bridges T, Young LS, Hall A. Activation of the small GTPase Cdc42 by the inflammatory cytokines TNF(alpha) and IL-1, and by the Epstein-Barr virus transforming protein LMP1. J Cell Sci. 1999 Sep;112 (Pt 17):2983-92.
6. Stengel K, Zheng Y. Cdc42 in oncogenic transformation, invasion, and tumorigenesis. Cell Signal. 2011 Sep;23(9):1415-23.
7. Garcia-Mata R, Boulter E, Burridge K. The 'invisible hand': regulation of RHO GTPases by RHOGDIs. Nat Rev Mol Cell Biol. 2011 Aug;12(8):493-504.
8. Micheau O, Tschopp J. Induction of TNF receptor I-mediated apoptosis via two sequential signaling complexes. Cell. 2003 Jul 25;114(2):181-90.
9. Bertrand MJ, Milutinovic S, Dickson KM, Ho WC, Boudreault A, Durkin J, et al. cIAP1 and cIAP2 facilitate cancer cell survival by functioning as E3 ligases that promote RIP1 ubiquitination. Mol Cell. 2008 Jun 20;30(6):689-700.
10. Dynek JN, Goncharov T, Dueber EC, Fedorova AV, Izrael-Tomasevic A, Phu L, et al. c-IAP1 and UbcH5 promote K11-linked polyubiquitination of RIP1 in TNF signalling. Embo J. 2010 Dec 15;29(24):4198-209.
11. Haas TL, Emmerich CH, Gerlach B, Schmukle AC, Cordier SM, Rieser E, et al. Recruitment of the linear ubiquitin chain assembly complex stabilizes the TNF-R1 signaling complex and is required for TNF-mediated gene induction. Mol Cell. 2009 Dec 11;36(5):831-44.
12. Varfolomeev E, Goncharov T, Fedorova AV, Dynek JN, Zobel K, Deshayes K, et al. c-IAP1 and c-IAP2 are critical mediators of tumor necrosis factor alpha (TNFalpha)-induced NF-kappaB activation. J Biol Chem. 2008 Sep 5;283(36):24295-9.
13. Silke J. The regulation of TNF signalling: what a tangled web we weave. Curr Opin Immunol. 2011 Oct;23(5):620-6.
14. Feoktistova M, Geserick P, Kellert B, Dimitrova DP, Langlais C, Hupe M, et al. cIAPs block Ripoptosome formation, a RIP1/caspase-8 containing intracellular cell death complex differentially regulated by cFLIP isoforms. Mol Cell. 2011 Aug 5;43(3):449-63.
15. Wang L, Du F, Wang X. TNF-alpha induces two distinct caspase-8 activation pathways. Cell. 2008 May 16;133(4):693-703.
16. Vanlangenakker N, Vanden Berghe T, Bogaert P, Laukens B, Zobel K, Deshayes K, et al. cIAP1 and TAK1 protect cells from TNF-induced necrosis by preventing RIP1/RIP3-dependent reactive oxygen species production. Cell Death Differ. 2011 Apr;18(4):656-65.
17. Vince JE, Wong WW, Khan N, Feltham R, Chau D, Ahmed AU, et al. IAP Antagonists Target cIAP1 to Induce TNFalpha-Dependent Apoptosis. Cell. 2007 Nov 16;131(4):682-93.
18. Gyrd-Hansen M, Darding M, Miasari M, Santoro MM, Zender L, Xue W, et al. IAPs contain an evolutionarily conserved ubiquitin-binding domain that regulates NF-kappaB as well as cell survival and oncogenesis. Nat Cell Biol. 2008 Nov;10(11):1309-17.

19. Lopez J, John SW, Tenev T, Rautureau GJ, Hinds MG, Francalanci F, et al. CARD-Mediated Autoinhibition of cIAP1's E3 Ligase Activity Suppresses Cell Proliferation and Migration. Mol Cell. 2011 May 4;42:569-83.
20. Gyrd-Hansen M, Meier P. IAPs: from caspase inhibitors to modulators of NF-kappaB, inflammation and cancer. Nat Rev Cancer. 2010 Aug;10(8):561-74.
21. Xu L, Zhu J, Hu X, Zhu H, Kim HT, LaBaer J, et al. c-IAP1 cooperates with Myc by acting as a ubiquitin ligase for Mad1. Mol Cell. 2007 Dec 14;28(5):914-22.
22. Cartier J, Berthelet J, Marivin A, Gemble S, Edmond V, Plenchette S, et al. Cellular inhibitor of apoptosis protein-1 (cIAP1) can regulate E2F1 transcription factor-mediated control of cyclin transcription. J Biol Chem. 2011 Jul 29;286(30):26406-17.
23. Zarnegar BJ, Wang Y, Mahoney DJ, Dempsey PW, Cheung HH, He J, et al. Noncanonical NF-kappaB activation requires coordinated assembly of a regulatory complex of the adaptors cIAP1, cIAP2, TRAF2 and TRAF3 and the kinase NIK. Nat Immunol. 2008 Dec;9(12):1371-8.
24. Vallabhapurapu S, Matsuzawa A, Zhang W, Tseng PH, Keats JJ, Wang H, et al. Nonredundant and complementary functions of TRAF2 and TRAF3 in a ubiquitination cascade that activates NIK-dependent alternative NF-kappaB signaling. Nat Immunol. 2008 Dec;9(12):1364-70.
25. Oberoi TK, Dogan T, Hocking JC, Scholz RP, Mooz J, Anderson CL, et al. IAPs regulate the plasticity of cell migration by directly targeting Rac1 for degradation. Embo J. 2011 Nov 25;31:14-28.
26. Varfolomeev E, Blankenship JW, Wayson SM, Fedorova AV, Kayagaki N, Garg P, et al. IAP antagonists induce autoubiquitination of c-IAPs, NF-kappaB activation, and TNFalpha-dependent apoptosis. Cell. 2007 Nov 16;131(4):669-81.
27. Boulter E, Garcia-Mata R, Guilluy C, Dubash A, Rossi G, Brennwald PJ, et al. Regulation of Rho GTPase crosstalk, degradation and activity by RhoGDI1. Nat Cell Biol. 2010 May;12(5):477-83.
28. Haubert D, Gharib N, Rivero F, Wiegmann K, Hosel M, Kronke M, et al. PtdIns(4,5)P-restricted plasma membrane localization of FAN is involved in TNF-induced actin reorganization. Embo J. 2007 Jul 25;26(14):3308-21.
29. Kant S, Swat W, Zhang S, Zhang ZY, Neel BG, Flavell RA, et al. TNF-stimulated MAP kinase activation mediated by a Rho family GTPase signaling pathway. Genes Dev. 2011 Oct 1;25(19):2069-78.
30. Van Troys M, Huyck L, Leyman S, Dhaese S, Vandekerkhove J, Ampe C. Ins and outs of ADF/cofilin activity and regulation. Eur J Cell Biol. 2008 Sep;87(8-9):649-67.
31. Iden S, Collard JG. Crosstalk between small GTPases and polarity proteins in cell polarization. Nat Rev Mol Cell Biol. 2008 Nov;9(11):846-59.
32. Etienne-Manneville S. Cdc42--the centre of polarity. J Cell Sci. 2004 Mar 15;117(Pt 8):1291-300.
33. Stengel KR, Zheng Y. Essential role of cdc42 in ras-induced transformation revealed by gene targeting. PLoS One. 2012;7(6):e37317.
34. Makrodouli E, Oikonomou E, Koc M, Andera L, Sasazuki T, Shirasawa S, et al. BRAF and RAS oncogenes regulate Rho GTPase pathways to mediate migration and invasion properties in human colon cancer cells: a comparative study. Mol Cancer. 2011;10:118-38.
35. Cheng CM, Li H, Gasman S, Huang J, Schiff R, Chang EC. Compartmentalized Ras proteins transform NIH 3T3 cells with different efficiencies. Mol Cell Biol. 2011 Mar;31(5):983-97.
36. Qiu RG, Abo A, McCormick F, Symons M. Cdc42 regulates anchorage-independent growth and is necessary for Ras transformation. Mol Cell Biol. 1997 Jun;17(6):3449-58.
37. Reymond N, Im JH, Garg R, Vega FM, Borda d'Agua B, Riou P, et al. Cdc42 promotes transendothelial migration of cancer cells through beta1 integrin. The Journal of cell biology. [Research Support, Non-U.S. Gov't]. 2012 Nov 12;199(4):653-68.
38. Gadea G, Roger L, Anguille C, de Toledo M, Gire V, Roux P. TNFalpha induces sequential activation of Cdc42- and p38/p53-dependent pathways that antagonistically regulate filopodia formation. J Cell Sci. 2004 Dec 15;117(Pt 26):6355-64.

39. Yang L, Wang L, Zheng Y. Gene targeting of Cdc42 and Cdc42GAP affirms the critical involvement of Cdc42 in filopodia induction, directed migration, and proliferation in primary mouse embryonic fibroblasts. Mol Biol Cell. 2006 Nov;17(11):4675-85.
40. Allen WE, Jones GE, Pollard JW, Ridley AJ. Rho, Rac and Cdc42 regulate actin organization and cell adhesion in macrophages. J Cell Sci. 1997 Mar;110 (Pt 6):707-20.
41. Fortin SP, Ennis MJ, Schumacher CA, Zylstra-Diegel CR, Williams BO, Ross JT, et al. Cdc42 and the guanine nucleotide exchange factors Ect2 and trio mediate Fn14-induced migration and invasion of glioblastoma cells. Mol Cancer Res. 2012 Jul;10(7):958-68.
42. Boulter E, Estrach S, Garcia-Mata R, Feral CC. Off the beaten paths: alternative and crosstalk regulation of Rho GTPases. FASEB J. 2012 Feb;26(2):469-79.
43. Geisbrecht ER, Montell DJ. A role for Drosophila IAP1-mediated caspase inhibition in Rac-dependent cell migration. Cell. 2004 Jul 9;118(1):111-25.
44. Liu J, Zhang D, Luo W, Yu Y, Yu J, Li J, et al. X-linked inhibitor of apoptosis protein (XIAP) mediates cancer cell motility via Rho GDP dissociation inhibitor (RhoGDI)-dependent regulation of the cytoskeleton. J Biol Chem. 2011 May 6;286(18):15630-40.
45. Zhuang M, Guan S, Wang H, Burlingame AL, Wells JA. Substrates of IAP Ubiquitin Ligases Identified with a Designed Orthogonal E3 Ligase, the NEDDylator. Mol Cell. 2013 Jan 24;49(2):273-82.
46. Dogan T, Harms GS, Hekman M, Karreman C, Oberoi TK, Alnemri ES, et al. X-linked and cellular IAPs modulate the stability of C-RAF kinase and cell motility. Nat Cell Biol. 2008 Dec;10(12):1447-55.
47. Hehnly H, Xu W, Chen JL, Stamnes M. Cdc42 regulates microtubule-dependent Golgi positioning. Traffic. 2010 Aug;11(8):1067-78.
48. Mace PD, Smits C, Vaux DL, Silke J, Day CL. Asymmetric recruitment of cIAPs by TRAF2. J Mol Biol. 2010 Jul 2;400(1):8-15.
49. Grandclement C, Pallandre JR, Valmary Degano S, Viel E, Bouard A, Balland J, et al. Neuropilin-2 expression promotes TGF-beta1-mediated epithelial to mesenchymal transition in colorectal cancer cells. PLoS One. 2011;6(7):e20444.

Figure legends

Figure 1. The organization of actin-cytokeleton is altered in cIAP1$^{-/-}$ MEFs. (**A**) Microscopic analysis of serum-starved wt or cIAP1$^{-/-}$ MEFs. Left panel: phase contrast images. Right panel: F-actin staining using AlexaFluor488-conjugated Phalloidin. (**B**) Filopodia-like structures were quantified by counting cells showing more than five filopodia-like. > 100 cells were analyzed. The mean reflects ± sd of at least three independent experiments. Statistical analysis was performed using the student's *t*-test. ***: p<0.001; **: p<0.01; *: p<0.05. (**C**) The expression of cIAP1 or cIAP1 mutants, cdc42-N17, IκB-super-repressor (SR), and the efficiency of control (si-Co) or NIK-targeted siRNAs (si-NIK) were checked by a western blot analysis. HSC70 was used as the loading control.

Figure 2. cIAP1 controls cdc42 stability. (A) Immunoblot analysis of cdc42, Rac1 and RhoA in MEFs from wt or cIAP1-deleted mice, treated or not with 40µM MG132 for 4hrs. HSC70 was used as the loading control. (**B**) Immmunoblot analysis of cdc42 in NIH3T3 cells transfected with cIAP1 targeting siRNA and treated or not with 40µM MG132 for 4hrs. Activated GTP-bound cdc42 was pulled-down using GST-PAK1-CRIB domain before immunoblot analysis. HSC70 was used as the loading control. (**C**) Immunoblot analysis of total or GTP-bound cdc42, and total and phosphorylated form of PAK1 in wt or cIAP1$^{-/-}$ MEFs. HSC70 was used as the loading control. Upper panel: The ratio GTP-bound/total cdc42 as quantified by a densitometric analysis of immunoblot. The mean reflects +/- sd of three independent experiments. (**D**) Western blot analysis of total or GTP-bound cdc42 and RhoGDIα in NIH3T3 transfected with cIAP1 encoding vector. HSC70 was used as the loading control. (**E**) Immunoblot analysis of cdc42, RhoGDIα and cIAP1 in MEFs from cIAP1-deleted mice transfected with control or cIAP1 encoding vector plus control or RhoGDIα-targeting siRNA. HSC70 was used as the loading control. (**F**) Immunoblot analysis of cIAP1 and cdc42 in cytosolic (Cyto) and membrane (Mb)-enriched fractions from cIAP1-deleted mice transfected with control or cIAP1-encoding vector. GM130 was used as a control for membrane-enrichment and HSC70 was used as the loading control. Right panel: The ratio cytosolic/membrane cdc42 expression as quantified by a densitometric analysis of immunoblots. The mean reflects +/- sd of two independent experiments. (**G**) Overexpression of cIAP1 increases the cdc42-RhoGDIα interaction. HEK293T were transfected with HA-cdc42 with or without cIAP1 encoding vectors. RhoGDIα was immunoprecipitated and co-precipitated and revealed by immunobloting using indicated antibodies.

Figure 3. cIAP1 can interact with cdc42. (A-C, F) GST-pull-down assay. (**A**) Cell lysates from HEK293T cells transfected with FLAG or FLAG-cIAP1 encoding vector were deposited onto GST-RhoA, -Rac1 or -cdc42 proteins. Interactions were analysis by immunobloting analysis using anti-cIAP1 specific antibody. (**B**) Lysates from HEK293T cells transfected with GFP-cdc42 encoding vector were incubated with GST-cIAP1 construct fusion proteins as indicated. Interactions were analyzed by a western blot using anti-GFP, anti-TRAF2 or anti-GST antibodies. (**C**) GST-cdc42 was immobilized onto glutathione sepharose beads and charged with GDP or GTP before incubating with HEK293T cell lysates. Interactions were revealed by immunoblotting using specific ant-cIAP1 or anti-PAK1 antibodies. (**D**) Surface Plasmon Resonance (Biacore) analysis of the interaction the BIR domains of cIAP1 with uncharged, GDP and GTP-charged cdc42 recombinant protein. (**E**) Co-immunoprecipitation analysis of the interaction of HA-cdc42 with cIAP1, TRAF2 and RhoGDI in HEK293T cells transfected with HA-cdc42. Interactions were revealed by immunobloting using

indicated antibodies. (**F**) Recombinant cIAP1 or TRAF2 were incubated with GST-cdc42 immobilized on glutathione sepharose beads. Interactions were evaluated by cIAP1 or TRAF2 immunoblotting.

Figure 4. Silencing of cIAP1 inhibits TNF-mediated Filopodia formation. NIH3T3 fibroblasts were transfected with control (si-Co) or cIAP1 (si-cIAP1) targeting siRNAs, serum starved for 16 hours and stimulated for an indicated time with 100ng/mL TNF. (**A&B)** Immunoflorescence analysis of F-actin staining was conducted using AlexaFluor488-conjugated Phalloidin. Filopodia were quantified by counting cells harboring more than 5 filopodia (B). > 100 cells were analyzed. The mean reflects ± sd of at least three independent experiments. Statistical analysis was performed using the student's *t*-test. ***: p=0.004; *: p=0.028. (**C**) Western blot analysis of cdc42 and Rac1, total and phosphorylated forms of cofilin and GSK3α and β. Activated GTP-bound cdc42 and Rac1 were pulled down using GST-PAK1-CRIB domain before immunoblot analysis. One representative experiment is shown. HSC70 was used as the loading control.

Figure 5. TNF-mediated filopodia formation is impaired in MEF cIAP1$^{-/-}$. MEF wt, cIAP1$^{-/-}$ (A, B, D-F) or cIAP1$^{-/-}$/cIAP2$^{-/-}$ (C) were serum starved for 16 hours, then stimulated for 10 minutes with 100ng/mL TNF. (**A**) Microscopic analysis of F-actin stained using AlexaFluor488-conjugated Phalloidin. (**B)** The number of filopodia per cells was counted. > 100 cells were analyzed. One representative experiment is shown. **(C)** Filopodia in cIAP1/cIAP2 double knock-out MEFs were detected as in A and counted. > 100 cells were analyzed. Results were expressed as fold filopodia induction/untreated cells (UT). The mean ± sd reflects at least three independent experiments. The expression of cIAP1 and cIAP2 is checked by immunobloting analysis (right panel). (**D-F**) Wt or cIAP1$^{-/-}$ MEFs were transfected with encoding plasmid vector (**D & E**) or si-RNAs (**F**), serum starved and treated for 10 minutes with 100ng/mL TNF. The expression of the constructs and the silencing efficiency were checked by immunobloting analysis (D, F: lower panel). Filopodia were detected as in A and counted (E, F). > 100 cells were analyzed. Results were expressed as fold filopodia induction/untreated cells (UT). The mean ± sd reflects at least three independent experiments (D & E). Statistical analysis was performed using the student's *t*-test. ***: p<0.001; **: p<0.01; *: p<0.05. N> 5 (D) or N=3 (E).

Figure 6. Deletion of cIAP1 prevents cdc42 activation. (**A**) Immunobloting analysis of cdc42, Rac1 and RhoA, in MEFs from wt or cIAP1-deleted mice. Cells were serum starved for 16 hours, then stimulated for 10 minutes with 100ng/mL TNF or EGF or 10% FBS as indicated. Activated GTP-bound cdc42 and Rac1 were pulled-down with GST-PAK1-CRIB domain and GTP-RhoA with a GST-Rhotekin-Rho binding domain before immunoblot analysis. One representative experiment is shown. The ratio GTP-bound/total GTPases is evaluated by a densitometric analysis of shown immunoblot. Because of the differential basal level of expression of cdc42 as observed in Figure 3, cell lysates from wt and cIAP1$^{-/-}$ MEFs were deposited onto separate gel and revealed separately. (**B**) Immunobloting analysis of cdc42 (GTP-bound and total) and PAK1 (phosphorylated form and total) in NIH3T3 cells transfected with cIAP1^{L47A} encoding plasmid vector 24 hours before serum starvation. Cells were stimulated for 10 minutes or indicated time with 100ng/mL TNF. HSC70 was used as a loading control. (**C)** HEK293T cells were transfected with HA-cdc42 and FLAG-cIAP1 and treated or not for 10 minutes with 100ng/mL TNF. Immunoprecipitation was performed using an anti-HA antibody and interactions were revealed by immunoblotting using anti-cIAP1, TRAF2 and HA antibodies.

Figure 7. cIAP1 regulates cdc42 functions. (**A**) NIH3T3 cells were transfected with control or cIAP1-targeting siRNA. Wound healings were induced by scratching the cell monolayer with a pipet tip.

Golgi-apparatus staining (red) were performed in NIH3T3 cells and wt and cIAP1$^{-/-}$ MEFs with an anti-GM130 and nucleus labeling with Hoechst five hours after scratching. Right panel. The percentage of cells with Golgi orientated toward the wound was quantified by counting at least 100 cells (mean +/- sd of three independent experiments). (**B**) Cdc42 activation in wt or cIAP1$^{-/-}$ MEFs transduced with HRas-V12 construct. Activated GTP-bound cdc42 was pulled-down with GST-PAK1-CRIB domain before immunobloting analysis. (**C)** Anchorage-independent growth of HRas-V12-infected wt or cIAP1$^{-/-}$ MEFs. Cells were cultured in soft-agar medium. The number of colonies was evaluated after ten days of culture. The T-test was used for statistical analysis (*, $P < 0.05$; N=5). (**D)** HRas-V12-infected wt or cIAP1$^{-/-}$ MEFs were injected subcutaneously in nude mice. The tumor was analyzed ten days later (two independent experiments are shown, n=5 per group). The Mann-Whitney test was used for statistical analysis (*: $p < 0.05$). (**E)** HRas-V12-infected wt or cIAP1$^{-/-}$ MEFs were injected into the tail veins of nude mice. Lung cancer foci were quantified 2 weeks later (two independent experiments are shown, n=4 per group). The Mann-Whitney test was used for statistical analysis (***: $p = 0.0006$). (**F**) CSFE-labeled PC3 cells, transfected with control or cIAP1-targeting siRNAs, were added on HUVEC confluent monolayer. PC3 cell adhesion was quantified by flow-cytometry (mean +/- sd of two independent experiments) (left panel). The efficiency of siRNAs was checked by a western blot analysis. (Uper panel). PC3 cell intercalation was evaluated by counting cells that display a non-round shape and a low phase-bright by time-laps microscopy. (> 100 cells were analyzed. The mean reflects ± sd of at least three independent experiments) (Right panel). Statistical analysis was performed using an ANOVA test. (***: $p<0.001$; **: $0.001<p<0.01$. **G.** CFSE-labeled wt or cIAP1$^{-/-}$ MEFs, transduced or not with HRas-V12 construct, were added on HUVEC confluent monolayer. MEF adhesion (left panel) and intercalation (right panel) were evaluated as in F.

Figure 8. Model for the regulation of cdc42 by cIAP1/TRAF2. cIAP1 interacts with TRAF2 via the BIR1 (B1) domain and with cdc42 via the BIR2 (B2) domain. **1**) In resting cells, cIAP1 binds cdc42. It stabilizes its interaction with its regulator RhoGDIα and then regulates cdc42 activation. **2**) The recruitment of TRAF2/cIAP1 to the receptor after TNF stimulation releases cdc42 and makes easier its activation leading to cytoskeleton reorganization and filopodia formation. **3**) Depletion of cIAP1 induces a loss of control of cdc42 and increases the activation/degradation cycle, leading to cytoskeleton modifications and filopodia-like structure.

Figure 1

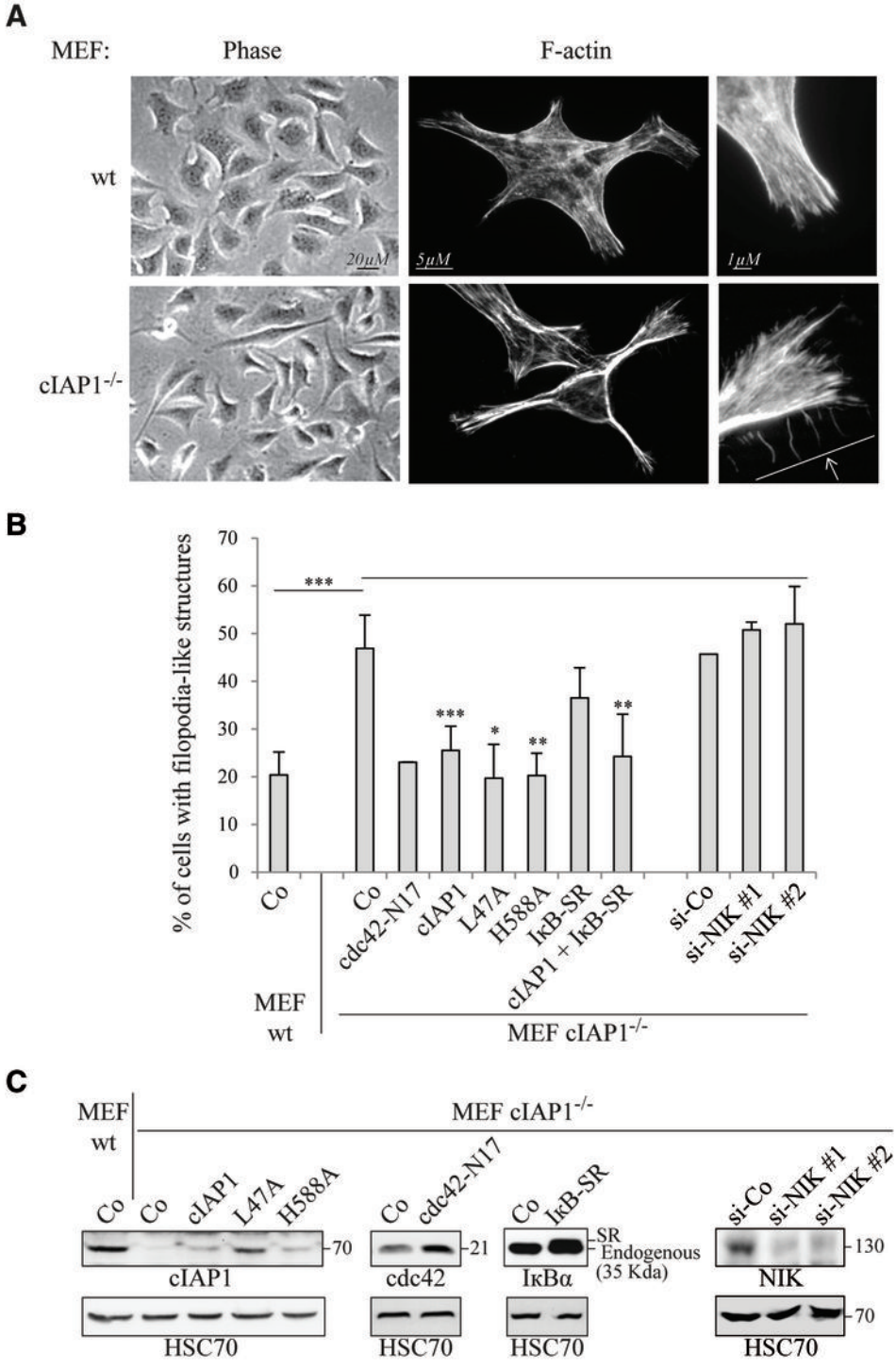
A
MEF:
Phase
F-actin
wt
cIAP1-/-
20μM
5μM
1μM
B
% of cells with filopodia-like structures
70
60
50
40
30
20
10
0
***
***
*
**
**
Co
Co
cdc42-N17
cIAP1
L47A
H588A
IκB-SR
cIAP1 + IκB-SR
si-Co
si-NIK #1
si-NIK #2
MEF wt
MEF cIAP1-/-
C
MEF wt
MEF cIAP1-/-
Co
Co
cIAP1
L47A
H588A
Co
cdc42-N17
Co
IκB-SR
si-Co
si-NIK #1
si-NIK #2
70
21
SR
Endogenous
(35 Kda)
130
cIAP1
cdc42
IκBα
NIK
HSC70
HSC70
HSC70
70
HSC70

Figure 2

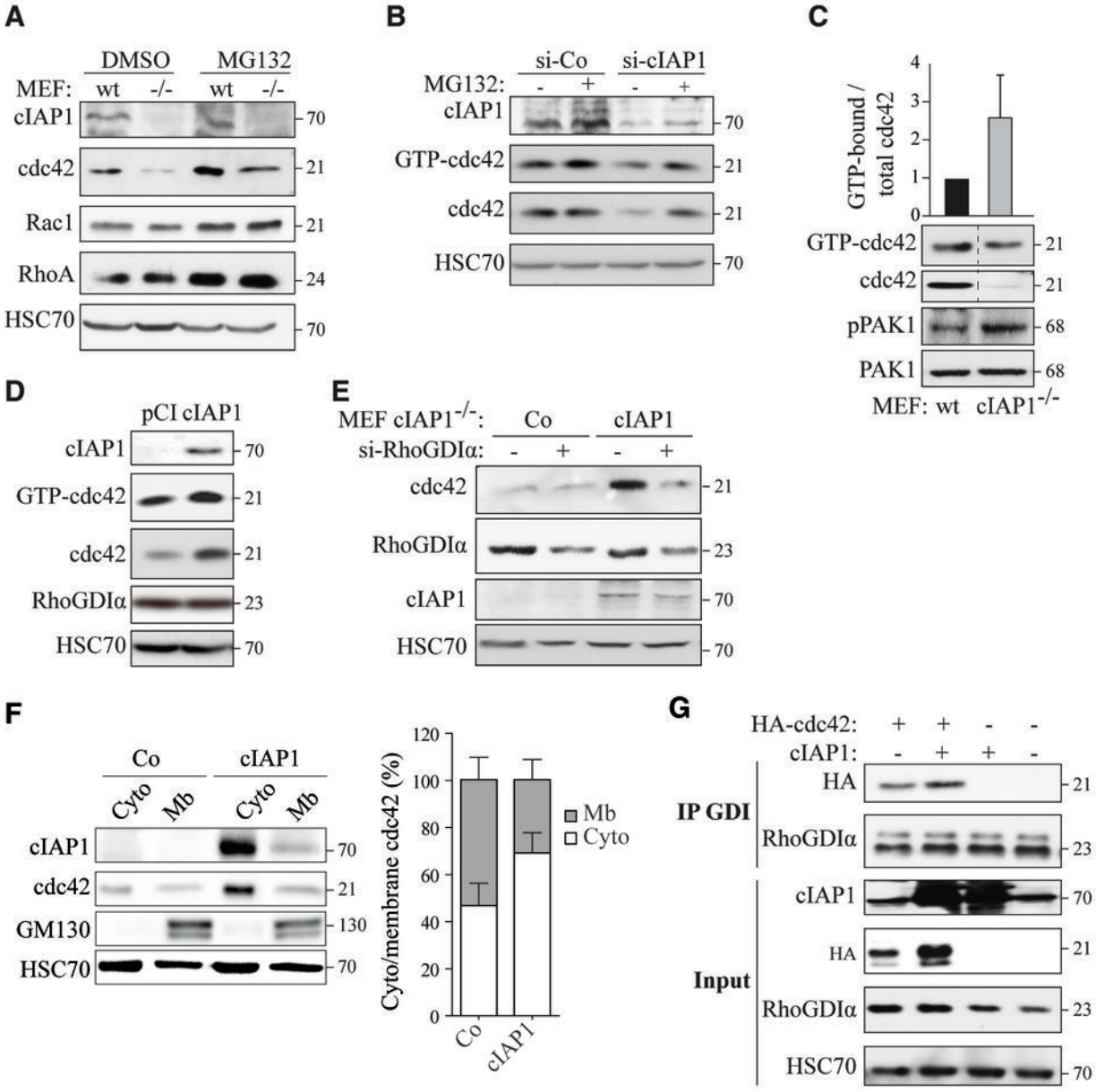
A
DMSO
MG132
MEF: wt -/- wt -/-
cIAP1
cdc42
Rac1
RhoA
HSC70
70
21
21
24
70
B
si-Co
si-cIAP1
MG132: - + - +
cIAP1
GTP-cdc42
cdc42
HSC70
70
21
21
70
C
GTP-bound / total cdc42
4
3
2
1
0
GTP-cdc42
cdc42
pPAK1
PAK1
21
21
68
68
MEF: wt cIAP1-/-
D
pCI cIAP1
cIAP1
GTP-cdc42
cdc42
RhoGDIα
HSC70
70
21
21
23
70
E
MEF cIAP1-/-: Co cIAP1
si-RhoGDIα: - + - +
cdc42
RhoGDIα
cIAP1
HSC70
21
23
70
70
F
Co
cIAP1
Cyto
Mb
Cyto
Mb
cIAP1
cdc42
GM130
HSC70
70
21
130
70
Cyto/membrane cdc42 (%)
120
100
80
60
40
20
0
Mb
Cyto
Co
cIAP1
G
HA-cdc42: + + - -
cIAP1: - + + -
IP GDI
HA
RhoGDIα
Input
cIAP1
HA
RhoGDIα
HSC70
21
23
70
21
23
70

Figure 3

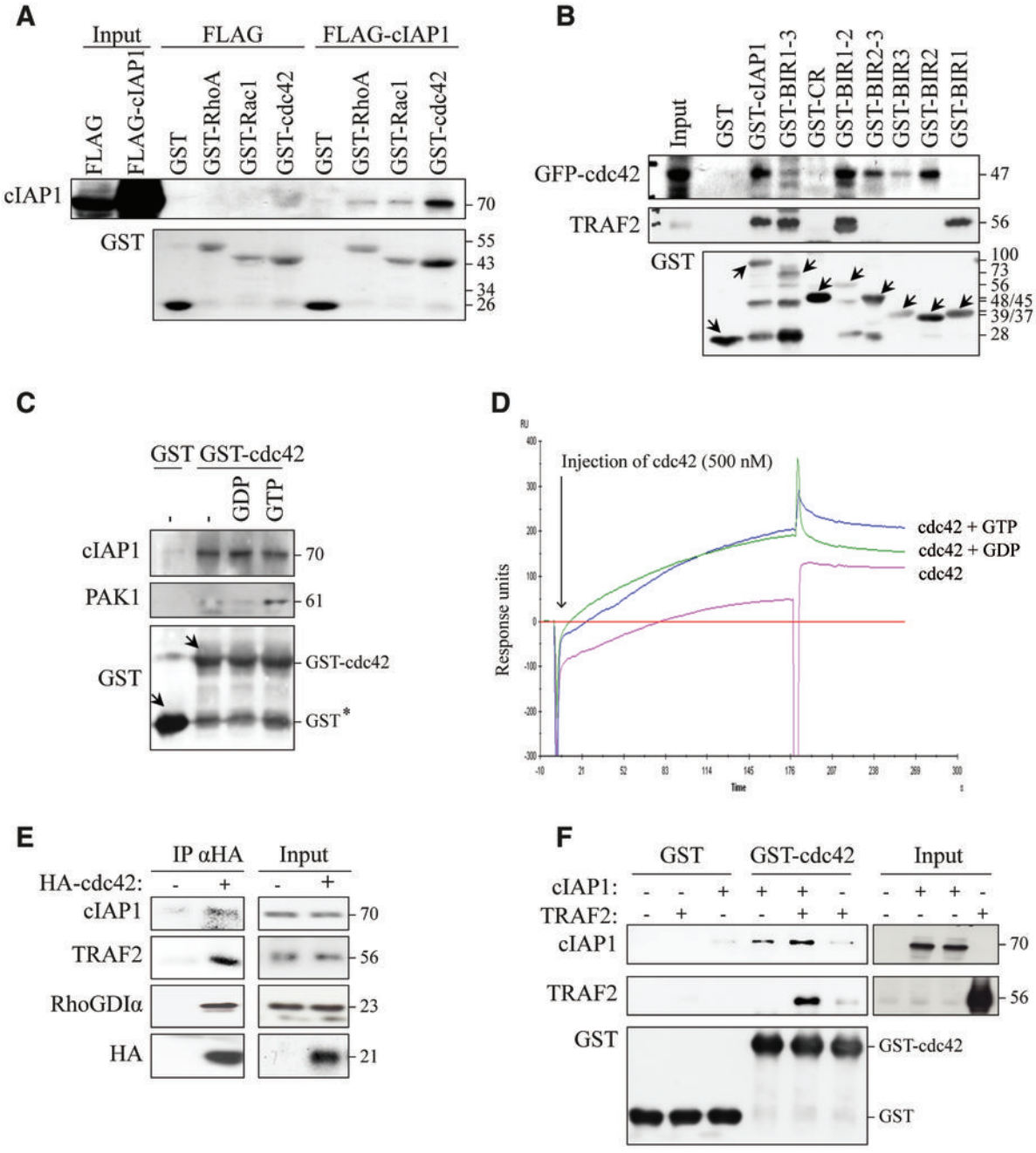
A
Input
FLAG
FLAG-cIAP1
FLAG
FLAG-cIAP1
GST
GST-RhoA
GST-Rac1
GST-cdc42
GST
GST-RhoA
GST-Rac1
GST-cdc42
cIAP1
GST
70
55
43
34
26
B
Input
GST
GST-cIAP1
GST-BIR1-3
GST-CR
GST-BIR1-2
GST-BIR2-3
GST-BIR3
GST-BIR2
GST-BIR1
GFP-cdc42
TRAF2
GST
47
56
100
73
56
48/45
39/37
28
C
GST
GST-cdc42
-
-
GDP
GTP
cIAP1
PAK1
GST
70
61
GST-cdc42
GST*
D
Injection of cdc42 (500 nM)
Response units
Time
cdc42 + GTP
cdc42 + GDP
cdc42
E
IP αHA
Input
HA-cdc42:
-
+
-
+
cIAP1
TRAF2
RhoGDIα
HA
70
56
23
21
F
GST
GST-cdc42
Input
cIAP1:
TRAF2:
cIAP1
TRAF2
GST
70
56
GST-cdc42
GST

Figure 4

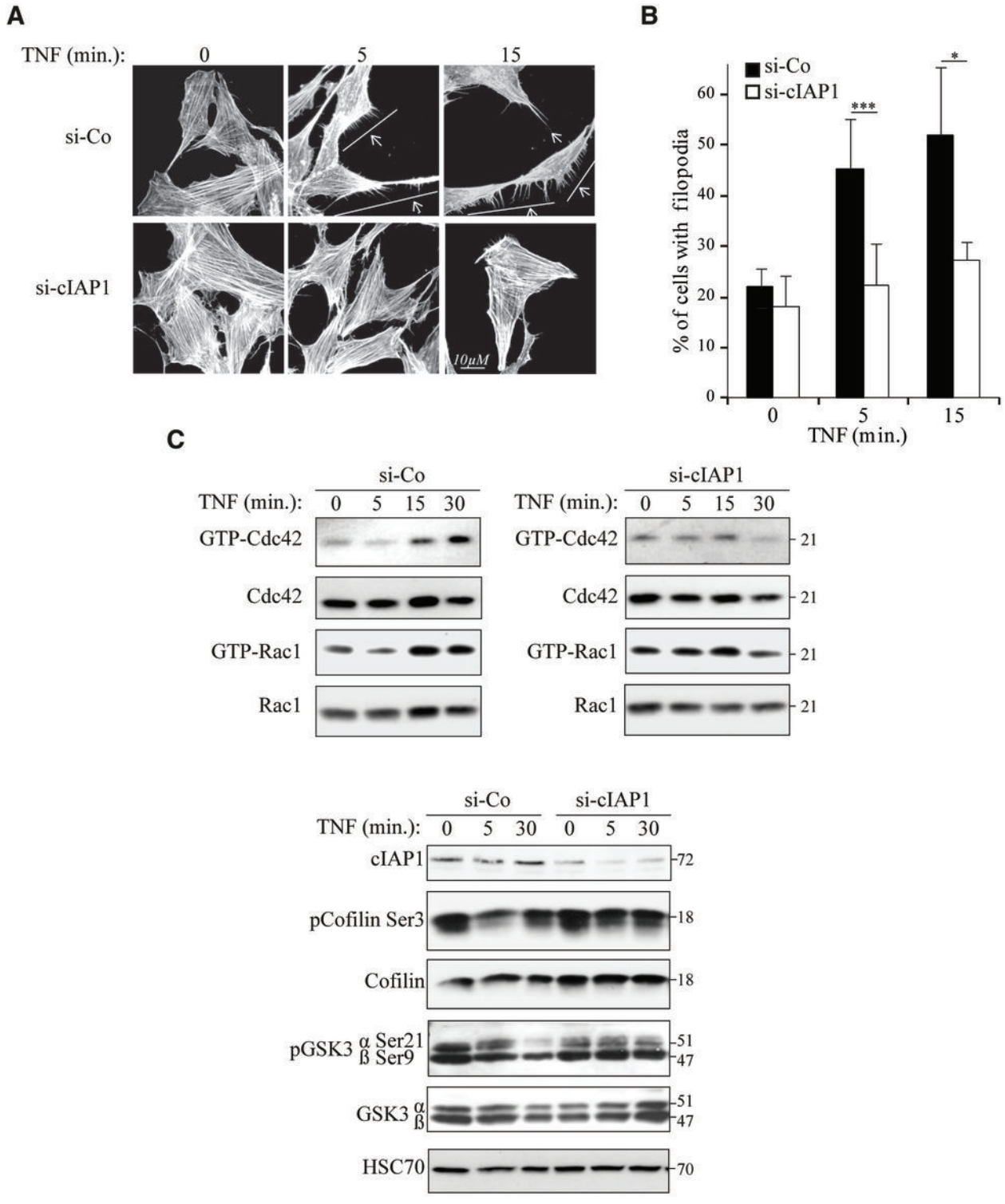
A
TNF (min.):
0
5
15
si-Co
si-cIAP1
10μM
B
si-Co
si-cIAP1
***
*
% of cells with filopodia
0
10
20
30
40
50
60
0
5
15
TNF (min.)
C
si-Co
si-cIAP1
TNF (min.):
0 5 15 30
GTP-Cdc42
Cdc42
GTP-Rac1
Rac1
21
TNF (min.):
0 5 30
cIAP1
72
pCofilin Ser3
18
Cofilin
18
pGSK3 α Ser21
ß Ser9
51
47
GSK3 α
ß
51
47
HSC70
70

Figure 5

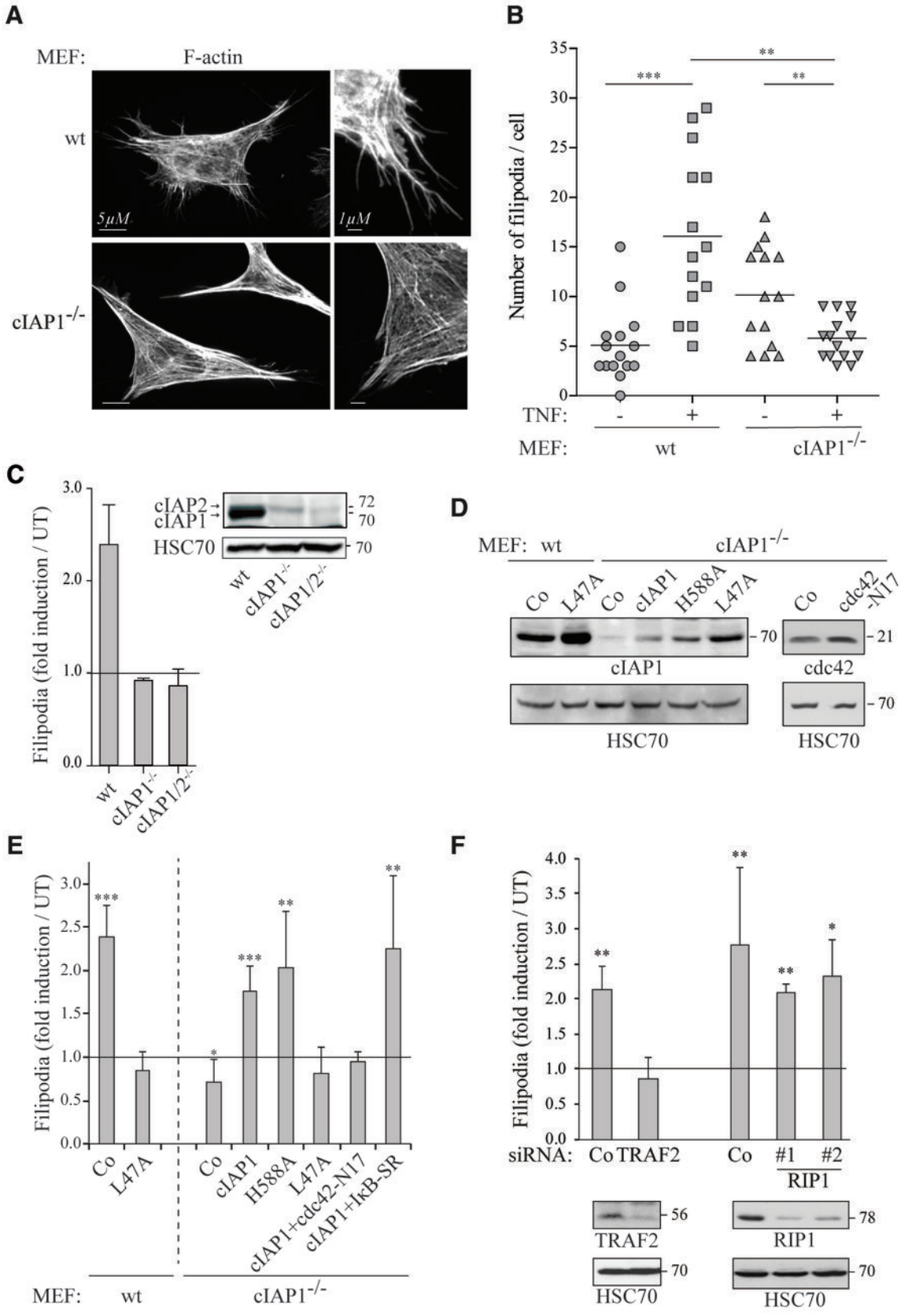
A
MEF:
F-actin
wt
cIAP1-/-
5μM
1μM
B
Number of filipodia / cell
TNF:
MEF:
wt
cIAP1-/-
C
Filipodia (fold induction / UT)
cIAP2
cIAP1
HSC70
72
70
wt
cIAP1-/-
cIAP1/2-/-
D
MEF: wt
cIAP1-/-
Co
L47A
cIAP1
H588A
cdc42 -N17
cdc42
HSC70
21
E
Filipodia (fold induction / UT)
Co
L47A
cIAP1
H588A
cIAP1+cdc42-N17
cIAP1+IκB-SR
MEF:
F
Filipodia (fold induction / UT)
siRNA:
Co
TRAF2
#1
#2
RIP1
TRAF2
RIP1
56
78

Figure 6

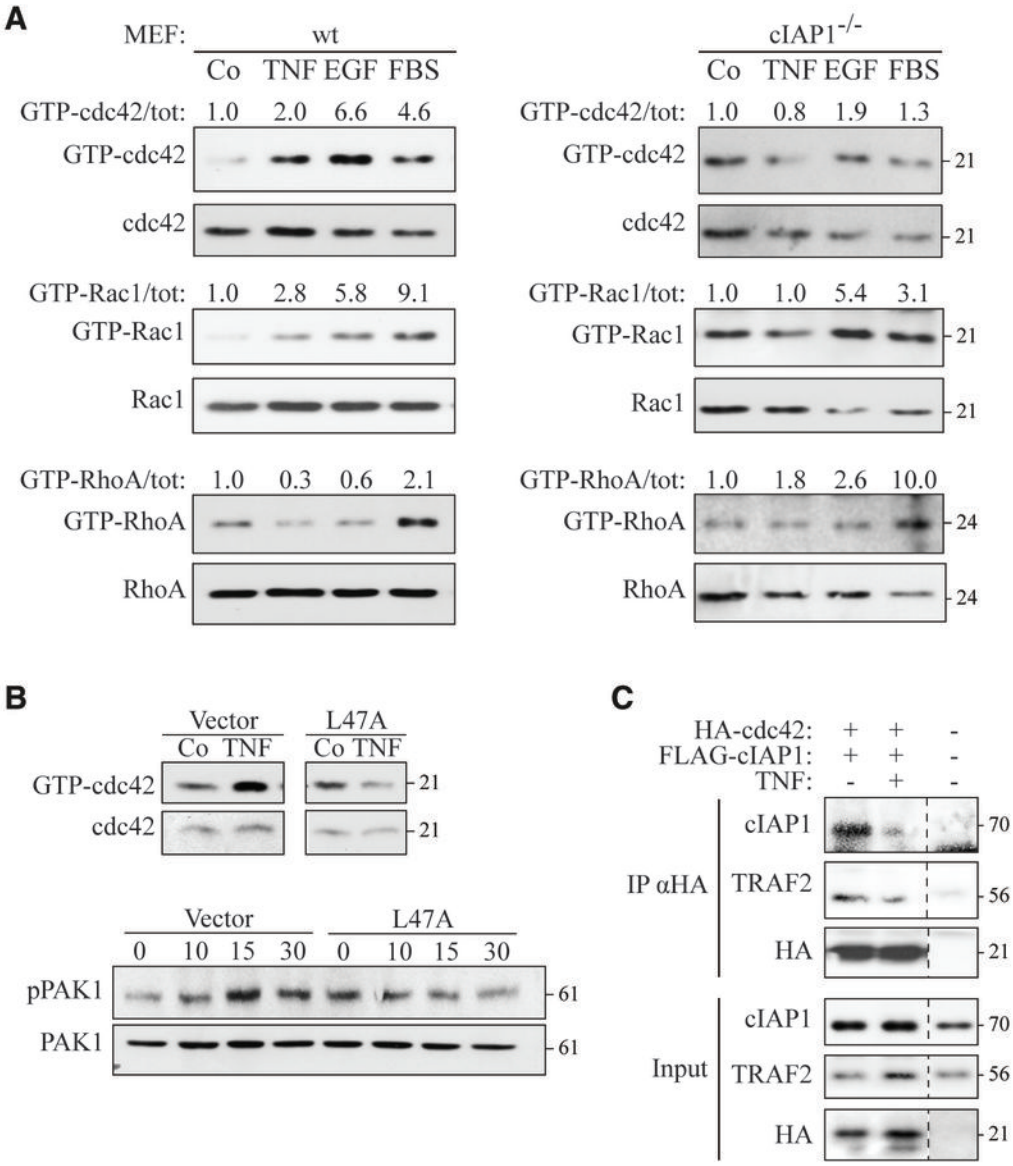
A
MEF:
wt
cIAP1-/-
Co TNF EGF FBS
GTP-cdc42/tot: 1.0 2.0 6.6 4.6
GTP-cdc42
cdc42
GTP-cdc42/tot: 1.0 0.8 1.9 1.3
GTP-Rac1/tot: 1.0 2.8 5.8 9.1
GTP-Rac1
Rac1
GTP-Rac1/tot: 1.0 1.0 5.4 3.1
GTP-RhoA/tot: 1.0 0.3 0.6 2.1
GTP-RhoA
RhoA
GTP-RhoA/tot: 1.0 1.8 2.6 10.0
21
24
B
Vector
L47A
Co TNF
GTP-cdc42
cdc42
0 10 15 30 0 10 15 30
pPAK1
PAK1
61
C
HA-cdc42: + + -
FLAG-cIAP1: + + -
TNF: - + -
IP αHA
Input
cIAP1
TRAF2
HA
70
56
21

Figure 7

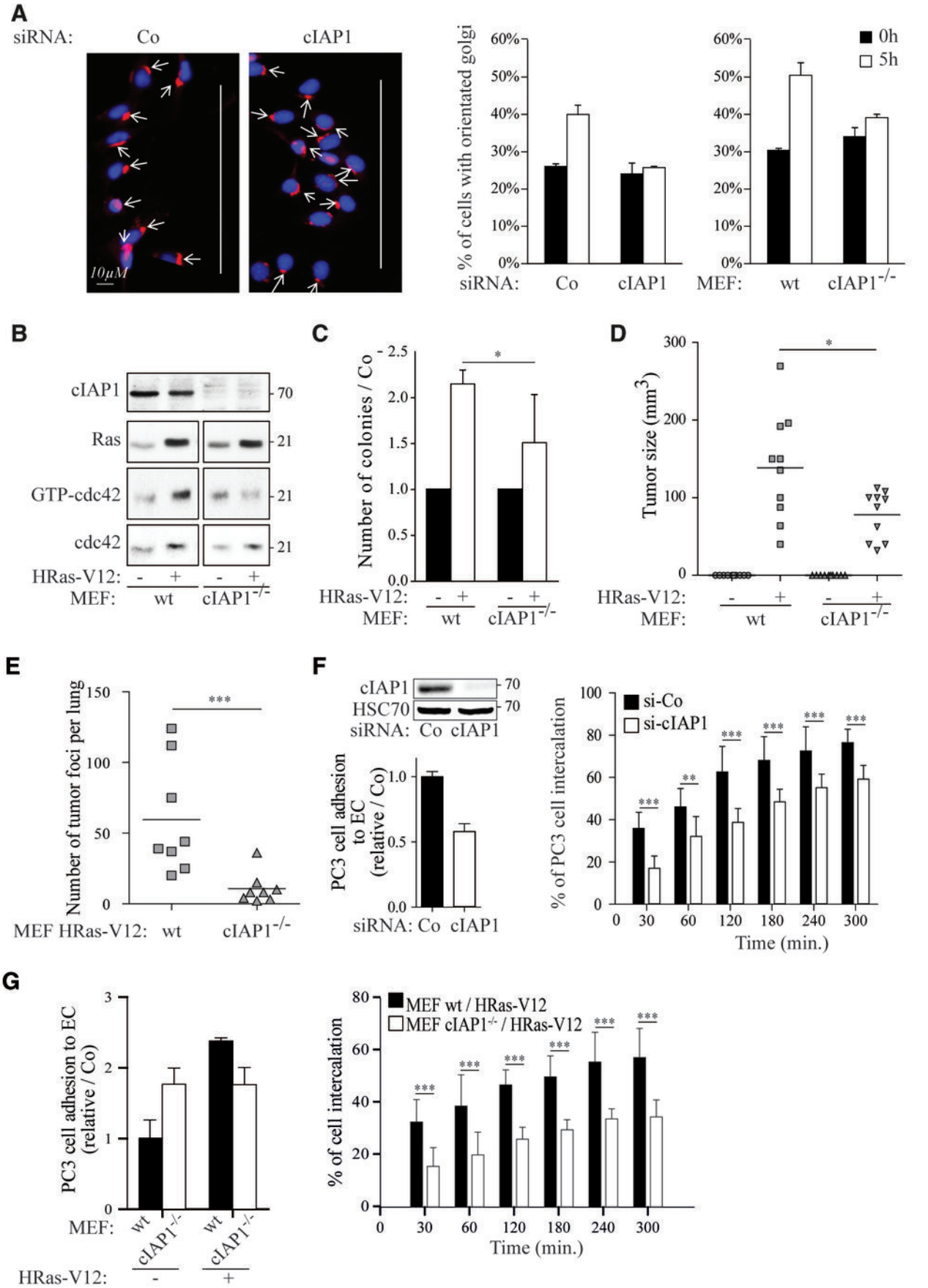
A
siRNA: Co cIAP1
10μM
% of cells with orientated golgi
0h
5h
siRNA: Co cIAP1
MEF: wt cIAP1-/-
B
cIAP1
Ras
GTP-cdc42
cdc42
HRas-V12:
MEF: wt cIAP1-/-
C
Number of colonies / Co
HRas-V12:
MEF: wt cIAP1-/-
D
Tumor size (mm3)
HRas-V12:
MEF: wt cIAP1-/-
E
Number of tumor foci per lung
MEF HRas-V12: wt cIAP1-/-
F
cIAP1
HSC70
siRNA: Co cIAP1
PC3 cell adhesion to EC (relative / Co)
si-Co
si-cIAP1
% of PC3 cell intercalation
Time (min.)
G
PC3 cell adhesion to EC (relative / Co)
MEF: wt cIAP1-/- wt cIAP1-/-
HRas-V12:
MEF wt / HRas-V12
MEF cIAP1-/- / HRas-V12
% of cell intercalation
Time (min.)

Figure 8

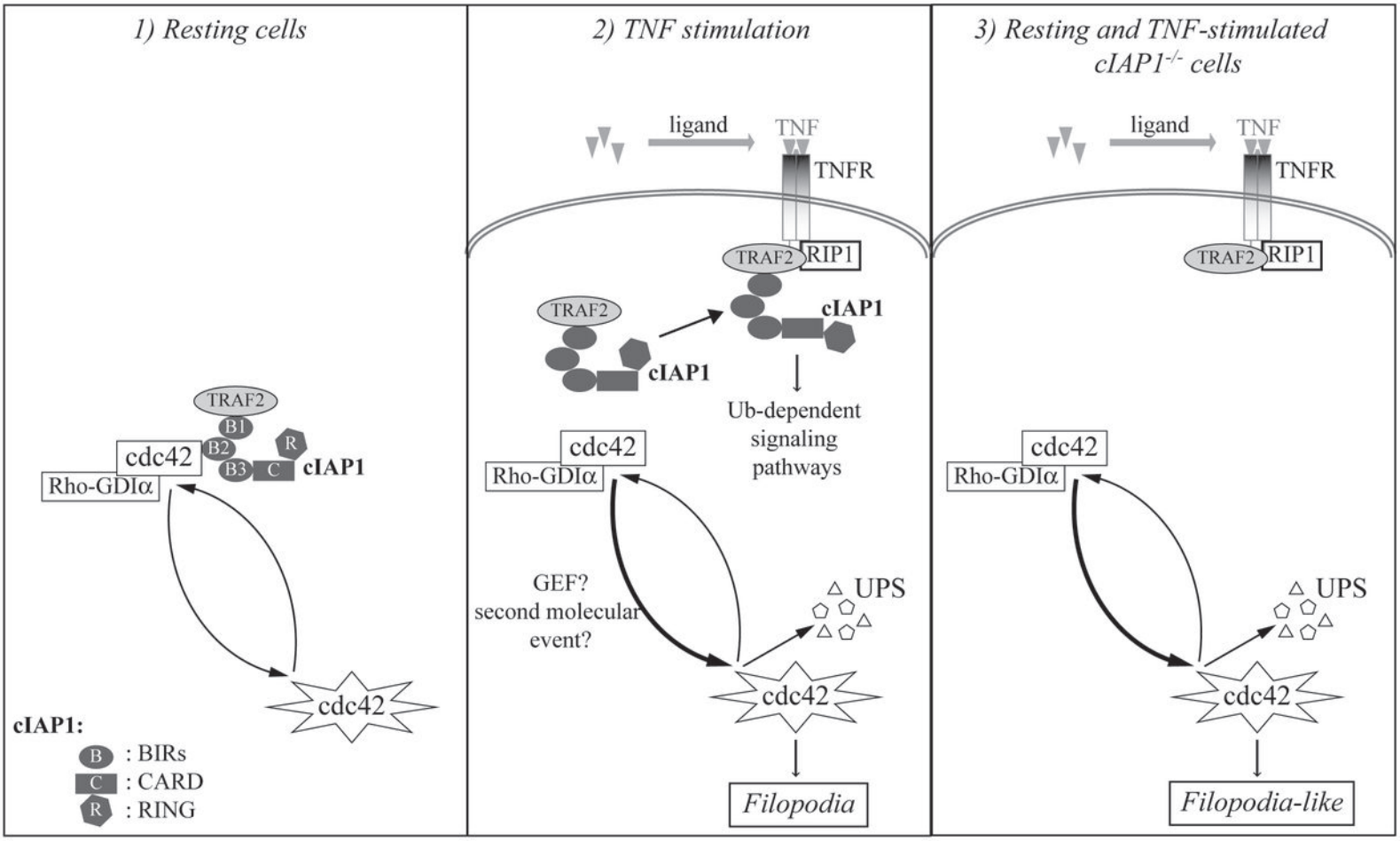
1) Resting cells
TRAF2
B1
B2
R
cdc42
B3
C
cIAP1
Rho-GDIα
cdc42
cIAP1:
B : BIRs
C : CARD
R : RING
2) TNF stimulation
ligand
TNF
TNFR
TRAF2
RIP1
TRAF2
cIAP1
cIAP1
Ub-dependent
signaling
pathways
cdc42
Rho-GDIα
GEF?
second molecular
event?
UPS
cdc42
Filopodia
3) Resting and TNF-stimulated
cIAP1-/- cells
ligand
TNF
TNFR
TRAF2
RIP1
cdc42
Rho-GDIα
UPS
cdc42
Filopodia-like